Real ray tracing in isotropic viscoelastic media: a numerical modelling

Václav Vavryčuk

Institute of Geophysics, Academy of Sciences, Boční II/1401, Praha 4, Czech Republic, E-mail: vv@ig.cas.cz

SUMMARY

The accuracy of the real ray tracing approach developed by Vavryčuk (2008a) for waves propagating in smooth inhomogeneous viscoelastic media is tested. The complex eikonal equation in isotropic viscoelastic media is solved using three alternative ray approaches: the real viscoelastic ray tracing, the real elastic ray tracing and the complex ray tracing. The first two approaches are simple but approximate. The complex ray tracing is complicated but yields the most accurate results, which serve as the reference solution. Two models of a smoothly inhomogeneous viscoelastic medium with high velocity gradients and with strong attenuation are used to check the robustness of the approximate methods. The numerical modelling reveals that the real viscoelastic ray approach is unequivocally preferable to the real elastic ray approach. It is more accurate and works even in situations when the elastic ray tracing fails. In the studied models, the errors in the complex traveltime produced by the real viscoelastic ray approach were 15 to 30 times less than those of the real elastic ray approach. Also the ray fields calculated by the real viscoelastic ray approach were excellently reproduced even in the case when the elastic rays yielded completely distorted results. Compared with the complex ray tracing, which is limited to simple types of media, the real viscoelstic ray tracing offers a fast and computationally undemanding procedure for calculating the complex travel times in complicated 3-D inhomogeneous attenuating structures.

1. INTRODUCTION

The ray theory is a powerful tool for solving wave propagation problems in complicated 3D inhomogeneous structures (Červený 2001). The ray-theoretical solution is a high-frequency approximation, which is frequently reasonably accurate and requires almost no computer time with respect to other numerical methods such as the finite differences or the finite elements (Moczo et al. 2004; Saenger & Bohlen 2004; Moczo et al. 2007). So far, the ray theory has mainly been applied to the wave propagation in elastic media, but in recent years

it was modified and extended also to media with attenuation (Caviglia & Morro 1992; Gajewski & Pšenčík 1992; Kiselev 1993; Ribodetti & Virieux 1998; Vavryčuk 2007a,b; Červený et al. 2008; Vavryčuk 2008a,b). The attenuation is incorporated into the modelling by substituting real elastic parameters by complex-valued and frequency-dependent viscoelastic parameters (Auld 1973; Carcione 1990; Carcione 2007). This causes that the basic ray equations become complex and their solution is sought in the complex space. The real ray theory valid in elastic media is thus substituted by the complex ray theory valid for viscoelastic media (Thomson 1997; Chapman et al. 1999; Hanyga & Seredyňska 1999, 2000; Kravtsov et al. 1999; Kravtsov 2005; Amodei et al. 2006).

The complex ray theory brings, however, complications. It is more computationally demanding than the real ray theory, because rays become curves in the complex space. Also building of the complex seismic model in the complex space brings difficulties, which prevent this theory to be extensively used in realistic applications. Therefore, Vavryčuk (2008a) proposed novel ray tracing equations (called real viscoelastic ray tracing equations) for solving the complex eikonal equation. The equations were derived from the Hamilton equations using a modified Hamiltonian. The ray tracing equations produce real-valued rays in contrast to the complex rays in the complex ray theory. However, the real viscoelastic ray approach is less accurate than the complex ray approach, and solves the complex eikonal equation only approximately.

In this paper, I perform numerical tests of the accuracy of the real viscoelastic ray approach developed by Vavryčuk (2008a). For a comparison, the complex eikonal equation is solved using two alternative ray approaches: the real elastic ray approach and the complex ray theory. The elastic ray approach is taken from Gajewski & Pšenčík (1992). It is simple and straightforward being applicable to weakly attenuating media. The rays are calculated in the elastic reference medium using the standard ray theory and attenuation effects are incorporated using perturbation formulas. For other more involved perturbation approaches, which use perturbation Hamiltonians of a different order, see Bulant & Klimeš (2002), Klimeš (2002), and Červený & Pšenčík (2008). Since the medium is chosen as very simple in the numerical tests, the complex eikonal equation is also solved using complex rays. The complex ray solution serves as the reference solution having the highest accuracy.

2. COMPLEX EIKONAL EQUATION

2.1. Notation

In formulas, the real and imaginary parts of complex-valued quantities are denoted by superscripts *R* and *I*, respectively. A complex-conjugate quantity is denoted by an asterisk.

The direction of a complex-valued vector **v** is calculated as $\mathbf{v}/\sqrt{\mathbf{v}^T\mathbf{v}}$, where the superscript T means the transposition. The magnitude of complex-valued vector **v** is complex valued and is calculated as $v=\sqrt{\mathbf{v}^T\mathbf{v}}$. If any complex-valued vector is defined by a real-valued direction, it is called homogeneous, and if defined by a complex-valued direction, it is called inhomogeneous. The directions of the real and imaginary parts of a complex-valued vector are parallel for a homogeneous vector but non-parallel for an inhomogeneous vector. The terms "homogeneous" and "inhomogeneous" are also used in the text to describe properties of the medium: elastic/viscoelastic parameters are constant in homogeneous media, but spatially dependent in inhomogeneous media. From the context, it is clear in which sense the terms "homogeneous/inhomogeneous" are used. In formulas, the Einstein summation convention is used for repeated subscripts.

2.2. Definition of the viscoelastic medium

An isotropic viscoelastic medium is defined by two complex-valued, frequency-dependent Lamé's coefficients

$$\lambda(\omega)=\lambda^R(\omega)+i\lambda^I(\omega),\ \mu(\omega)=\mu^R(\omega)+i\mu^I(\omega)\ . \tag{1}$$

The real parts of Lamé's coefficients, λ^R and μ^R, describe elastic properties of the medium, the imaginary parts, λ^I and μ^I, describe attenuation. The phase velocities for *P* and *S* waves calculated from λ and μ and from the density of the medium ρ,

$$c_P=\sqrt{\frac{\lambda+2\mu}{\rho}},\ c_S=\sqrt{\frac{\mu}{\rho}}, \tag{2}$$

are complex-valued and frequency-dependent. The strength of attenuation is evaluated using quality factor Q

$$Q=-\frac{\left(c^2\right)^R}{\left(c^2\right)^I}, \tag{3}$$

which reads for *P* and *S* waves

$$Q_P=-\frac{\lambda^R+2\mu^R}{\lambda^I+2\mu^I}\ ,\ Q_S=-\frac{\mu^R}{\mu^I}\ . \tag{4}$$

The sign in formulas (3) and (4) depends on the definition of the Fourier transform applied to calculating the viscoelastic parameters in the frequency domain. Here I use the forward Fourier transform with the exponential term $\exp(i\omega t)$, hence the quality factor is defined with the minus sign. If using the Fourier transform with the exponential term $\exp(-i\omega t)$, the minus sign must be omitted. For elastic media, the *Q*-factor is infinite.

2.3. Equation of motion in viscoelastic media

Equation of motion in viscoelastic media expressed in the frequency domain has the same form as in elastic media

$$\rho\omega^2 u_i + \sigma_{ij},_j = 0 \ , \tag{5}$$

where $\rho = \rho(\mathbf{x})$ is the density of the medium, $\mathbf{u} = \mathbf{u}(\mathbf{x}, \omega)$ is the displacement vector, $\sigma_{ij} = \sigma_{ij}(\mathbf{x}, \omega)$ is the stress tensor, $\mathbf{x}$ is the position vector, and ω is the circular frequency. Density ρ, position vector $\mathbf{x}$, and frequency ω are real-valued quantities, other quantities in (5) are complex. Absence of external forces is assumed in eq. (5). The stress tensor is defined in the frequency domain as

$$\sigma_{ij} = c_{ijkl} e_{kl} \ , \tag{6}$$

where $e_{kl} = e_{kl}(\mathbf{x}, \omega)$ are the components of the strain tensor

$$e_{kl} = \frac{1}{2}\left(u_k,_l + u_l,_k\right) \ , \tag{7}$$

and $c_{ijkl} = c_{ijkl}(\mathbf{x}, \omega)$ is the tensor of viscoelastic parameters. In isotropic media, c_{ijkl} is defined using complex-valued and frequency-dependent Lamé's coefficients λ and μ,

$$c_{ijkl} = \lambda\delta_{ij}\delta_{kl} + \mu\left(\delta_{ik}\delta_{jl} + \delta_{il}\delta_{jk}\right) . \tag{8}$$

2.4. Eikonal equation

Let us assume a high-frequency signal with displacement $\mathbf{u} = \mathbf{u}(\mathbf{x}, \omega)$ in the following form

$$u_i(\mathbf{x}, \omega) = U_i(\mathbf{x}) \exp[i\omega\tau(\mathbf{x})] = U_i(\mathbf{x}) \exp\left[-\omega\tau^I(\mathbf{x})\right] \exp\left[i\omega\tau^R(\mathbf{x})\right] \ , \tag{9}$$

where $\mathbf{U} = \mathbf{U}(\mathbf{x})$ is the complex-valued amplitude, and $\tau = \tau(\mathbf{x})$ is the complex-valued travel time. The real part of the traveltime, τ^R, describes the propagation time of the signal,

and the imaginary part, τ^I, describes the exponential decay of the signal amplitude along a ray due to attenuation. Inserting eq. (9) into equation of motion (5), we obtain the eikonal equation,

$$c^2 \frac{\partial \tau}{\partial x_i} \frac{\partial \tau}{\partial x_i} = 1 , \tag{10}$$

where c is the complex-valued phase velocity defined in eq. (2). Position vector **x** in (10) is real. Introducing the complex-valued slowness vector **p** as

$$p_i = \frac{\partial \tau}{\partial x_i} , \tag{11}$$

equation (10) reads

$$c^2 p_i p_i = 1 . \tag{12}$$

The slowness vector **p** can be decomposed into its real and imaginary parts, $\mathbf{p} = \mathbf{p}^R + i\mathbf{p}^I$, where

$$p_i^R = \frac{\partial \tau^R}{\partial x_i} \ , \quad p_i^I = \frac{\partial \tau^I}{\partial x_i} \ , \tag{13}$$

define the directions of the signal propagation and of the exponential amplitude decay, respectively. The eikonal equation can be rewritten in the following form (Červený 2001, eq. 3.6.3)

$$H(\mathbf{x}, \mathbf{p}) = \frac{1}{2}\left(c^2 p_i p_i - 1\right) = 0 \ , \tag{14}$$

where $H = H(\mathbf{x}, \mathbf{p})$ is the Hamiltonian, and vectors **x** and **p** are the generalized coordinates.

3. REAL VISCOELASTIC RAY TRACING IN VISCOELASTIC MEDIA

Vavryčuk (2008a) proposed a method of solving the complex eikonal equation using the real viscoelastic ray tracing method. In his approach, the Hamiltonian for viscoelastic media is modified in order to keep rays as trajectories in the real space. The imaginary part

of the slowness vector $\mathbf{p}^I$ is not an independent variable in the Hamiltonian equations as in the complex ray theory (see Section 4.1.), but it is calculated from the condition the complex-valued slowness vector to be stationary. This condition ensures that the complex energy velocity vector **v** is homogeneous and the ray direction is always real. The approach is developed for isotropic as well as anisotropic media. The stationary slowness vector is homogeneous in isotropic media but inhomogeneous in anisotropic media. In isotropic media, the ray tracing equations read (see Vavryčuk 2008a, eqs 39 and A7):

$$\frac{dx_i}{d\tau^R} = V^2 p_i^R, \quad \frac{dp_i^R}{d\tau^R} = -\frac{1}{V}\frac{\partial V}{\partial x_i}, \quad \frac{d\tau^I}{d\tau^R} = -\frac{c^I}{c^R}, \tag{15}$$

where V is the real-valued phase velocity calculated from the complex-valued phase velocity c as,

$$V = \frac{1}{\left(c^{-1}\right)^R}, \tag{16}$$

and τ^R and τ^I are the real and imaginary parts of the travel time τ. For the ray tracing equations in anisotropic viscoelastic media, see Vavryčuk (2008a, eqs 29 and 35). Equations (15) yield for τ^I

$$\tau^I = -\int_{\tau_0^R}^{\tau^R} \frac{c^I}{c^R} d\tau^R. \tag{17}$$

The imaginary part of slowness vector **p** is calculated as the gradient of τ^I,

$$p_i^I = \frac{\partial \tau^I}{\partial x_i}. \tag{18}$$

Note that the resultant slowness vector, $\mathbf{p} = \mathbf{p}^R + \mathbf{p}^I$, where $\mathbf{p}^R$ is calculated from (15) and $\mathbf{p}^I$ from (18), is no longer stationary. The condition of the stationary slowness vector was applied as an approximation when calculating **x** and $\mathbf{p}^R$ by eq. (15). After constructing the real ray fields, this approximation is replaced by a more correct procedure and $\mathbf{p}^I$ is calculated using eq. (18).

Having calculated the complex traveltme τ by (15) and (17), we can define isochrones and rays. The real and imaginary isochrones are formed by points of constant τ^R and τ^I, respectively. The propagation and attenuation rays are orthogonal curves to the

real and imaginary isochrones. If propagation and attenuation rays coincide, the complex slowness vector **p** is homogeneous. In most cases, however, the propagation and attenuation rays differ and vector **p** is inhomogeneous. The real and imaginary isochrones as well as the propagation and attenuation rays are curves defined in the real space.

Since the rays are forced to lie in the real space, the method is approximate. On the other hand, the real viscoelastic ray theory is simple and applicable to a broad family of models of the medium, and computational requirements are roughly the same as for the ray tracing in elastic media.

4. ALTERNATIVE RAY APPROACHES

4.1. Complex ray theory

The most straightforward way how to solve the complex eikonal equation (10) is to apply the method of characteristics using the complex Hamilton-Jacobi equations (Kravtsov 2005). Their form is quite analogous to the real Hamilton-Jacobi equations (Červený 2002, eq. 5)

$$\frac{dx_i}{d\sigma} = \frac{\partial H}{\partial p_i} \ , \quad \frac{dp_i}{d\sigma} = -\frac{\partial H}{\partial x_i} , \quad \frac{d\tau}{d\sigma} = p_i \frac{\partial H}{\partial p_i} \ , \tag{19}$$

where σ is a parameter along a ray. For $\sigma = \tau$ and H expressed in eq. (14), eq. (19) reads

$$\frac{dx_i}{d\tau} = c^2 p_i \ , \quad \frac{dp_i}{d\tau} = -\frac{1}{c}\frac{\partial c}{\partial x_i} \ , \tag{20}$$

being formally identical with the ray tracing equations in elastic media (Červený 2001, eq. 3.6.4). In the complex ray theory, however, all quantities in (20) become complex. It includes generalized coordinates $\mathbf{x} = \mathbf{x}^R + i\mathbf{x}^I$ and $\mathbf{p} = \mathbf{p}^R + i\mathbf{p}^I$, which form a 12 dimensional (12-D) phase space. The rays are trajectories in the complex space, and the solution of the ray tracing equations is sought in the 12-D **x**-**p** phase space. When solving the two-point ray tracing, the source and the receiver are positioned in the real space, but the ray connecting them is, generally, a curve in the complex space.

Finally, from the solution $\mathbf{x} = \mathbf{x}(\tau)$ obtained from (20), we invert for complex traveltime τ as a function of real space coordinates $\mathbf{x}^R$,

$$\tau = \tau\left(\mathbf{x}^R\right) . \tag{21}$$

Unfortunately, the complex ray tracing encounters difficulties. The complex ray theory is more computationally demanding than the real ray theory, because complex rays are curves in the 6-D space. However, the main difficulty is the model building, because the model must be defined in the complex space. The phase velocity c needed in (20) is measured in the real space, $c = c(\mathbf{x}^R)$, but it must be analytically continued to the complex space, $c = c(\mathbf{x})$. This can be done for homogeneous or smoothly inhomogeneous media, but so far it is unclear how to do it for 3-D inhomogeneous structures with interfaces. This restricts the applicability of the complex ray theory to simple media only.

Interestingly, the complex ray tracing equations have explicit analytical solutions in special cases. For example, the equations can be analytically solved for a medium with the constant gradient in c^{-2} (see Appendix A).

4.2. Elastic ray theory

The simplest method how to incorporate attenuation into the standard real ray theory is to consider a viscoelastic medium as the perturbation of a perfectly elastic medium. The rays are traced in the elastic reference medium and the effects of attenuation are calculated by the first-order perturbations (Gajewski & Pšenčík 1992; Vavryčuk 2008b). The ray tracing equations are identical with those for the elastic reference medium, only an additional equation for τ^I is supplemented,

$$\frac{dx_i}{d\tau^R} = V_0^2 p_i^R \ , \quad \frac{dp_i^R}{d\tau^R} = -\frac{1}{V_0}\frac{\partial V_0}{\partial x_i} \ , \quad \frac{d\tau^I}{d\tau^R} = -\frac{1}{2}\frac{\left(c^2\right)^I}{\left(c^2\right)^R} = \frac{1}{2}Q^{-1} \ . \tag{22}$$

Velocity V_0 is the real-valued reference velocity in the reference elastic medium,

$$V_0 = \sqrt{\left(c^2\right)^R} \ . \tag{23}$$

The imaginary traveltime τ^I is calculated from (22) by a quadrature along the reference ray

$$\tau^I = \frac{1}{2}\int_{\tau_0^R}^{\tau^R} Q^{-1} d\tau^R \ . \tag{24}$$

The imaginary part of slowness vector **p** is calculated as the gradient of τ^I.

This approach is approximate and works mostly for weakly attenuating media. Its accuracy can be enhanced by incorporating higher-order perturbations. Similarly as the real

viscoelastic ray approach described in Section 3, the elastic ray approach is applicable to a broad family of medium models, and the computational requirements are comparable with those of the ray tracing in elastic media.

When comparing eqs (15) and (22), we can see that the real elastic and viscoelastic ray approaches are similar. Both approaches solve **x,** $\mathbf{p}^R$ and τ^I as a function of τ^R and produce real rays. However, the computed ray fields and traveltime $\tau = \tau(\mathbf{x})$ are not identical. The differences are caused by a different definition of the real-valued phase velocity and by a different formula for calculating τ^I in (15) and (22). The differences are more pronounced in media with strong attenuation. In media with weak attenuation, they are of the order of the second and higher perturbations.

5. ACCURACY OF THE REAL RAY TRACING

In this section, I examine numerically the accuracy of the real ray tracing methods. I consider two models of the viscoelastic medium: model A and model B. Both models are smoothly inhomogeneous with a constant gradient of c^{-2}. For such models, an exact solution of the complex eikonal equation can be found analytically using the complex ray tracing (see Appendix A). The complex phase velocity c as a function of coordinates reads

$$c^{-2}(\mathbf{x}) = c_0^{-2} + A_i x_i \,, \tag{25}$$

where $c_0 = 1$, $A_1 = 0.1i$, $A_2 = 0$ and $A_3 = 0$ for model A, and $c_0 = 1$, $A_1 = 0.1i$, $A_2 = 0$ and $A_3 = -0.15$ for model B. The phase velocity c_0 is in km/s, the gradients A_i are in $\mathrm{s}^2/\mathrm{km}^3$. The eikonal equation is solved in the x-z plane for x between 0 and 10 km and for z between 0 and 4 km. For initial time $t = 0$, the complex traveltime τ is set to be zero for the whole region under study. The waves are excited by a point source situated at the origin of coordinates $\mathbf{x}_S = (0, 0)^T$.

The models A and B are artificial and probably do not reflect any seismic structure. The gradients of complex velocity c are very strong and behave independently for real and imaginary parts of c. In both models, the gradient in attenuation (gradient in c^I) is along the x axis. The Q-factor decreases from the value of $Q = \infty$ at $x = 0$ down to the value of $Q = 1$ at $x = 10$ km. Model B also displays a real vertical gradient in c^{-2}. In seismic structures, the attenuation and the real velocity gradients are not so strong and usually they are correlated. The high-velocity structures are associated with the low attenuation and vice versa. Here, the models are used just as extremes for checking the robustness of the real ray tracing methods. In real applications, the accuracy of the methods should be higher.

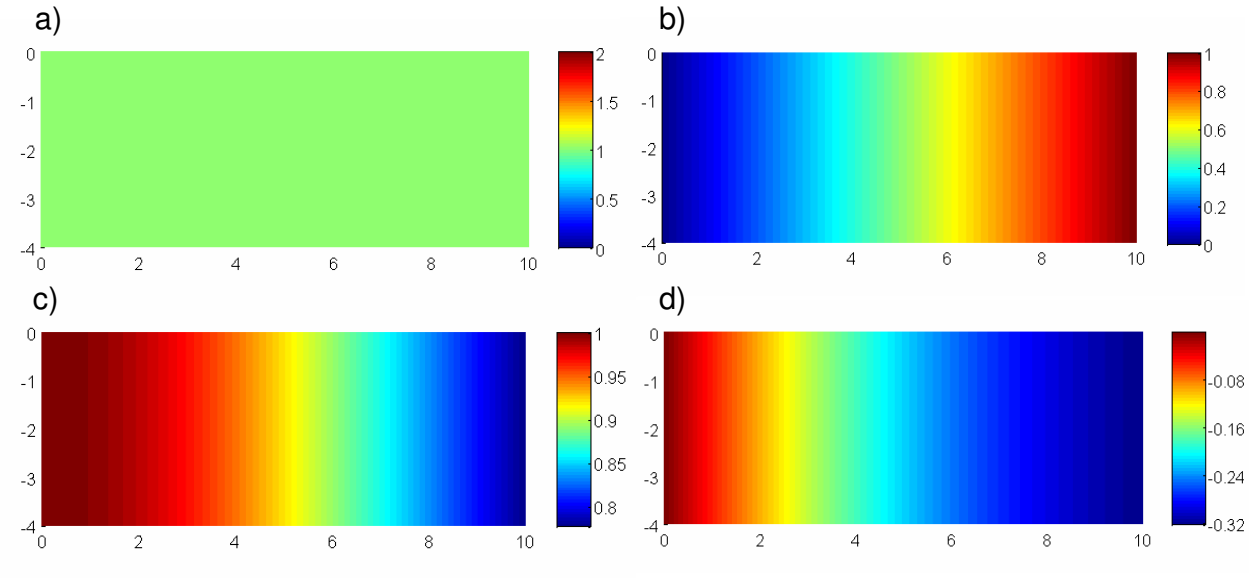

Figure 1. Real (a) and imaginary (b) parts of the square of slowness c^{-2}, and real (c) and imaginary (d) parts of complex phase velocity c in model A. The colour scales in (a) and (b) are in s^2/km^2, the colour scales in (c) and (d) are in km/s. The horizontal and vertical scales are in km.

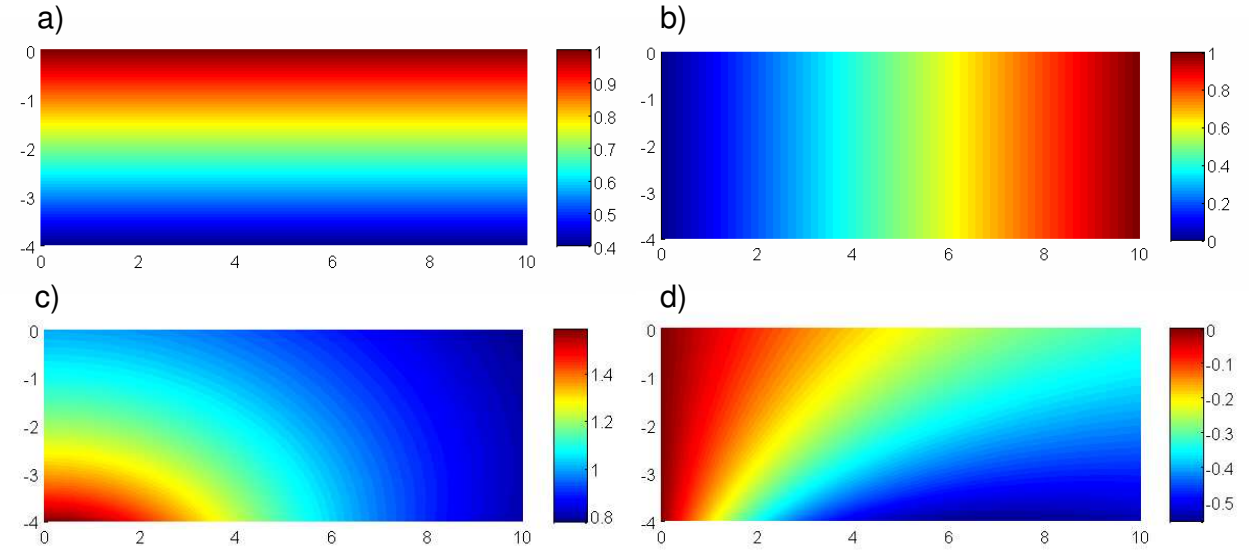

Figure 2. Real (a) and imaginary (b) parts of the square of slowness c^{-2}, and real (c) and imaginary (d) parts of complex phase velocity c in model B. The colour scales in (a) and (b) are in s^2/km^2, the colour scales in (c) and (d) are in km/s. The horizontal and vertical scales are in km.

Figures 1 and 2 display velocity models A and B, respectively. Plots (a) and (b) show the real and imaginary parts of the square of the complex slowness c^{-2}, plots (c) and (d) show the real and imaginary parts of the complex phase velocity c. Model A is simpler than model B because it is characterized only by the horizontal gradients in c^R and c^I. In model B, the real vertical gradient in c^{-2} and the imaginary horizontal gradient in c^{-2} superimpose and produce a complicated pattern in $c^R = c^R(x,z)$ and $c^I = c^I(x,z)$.

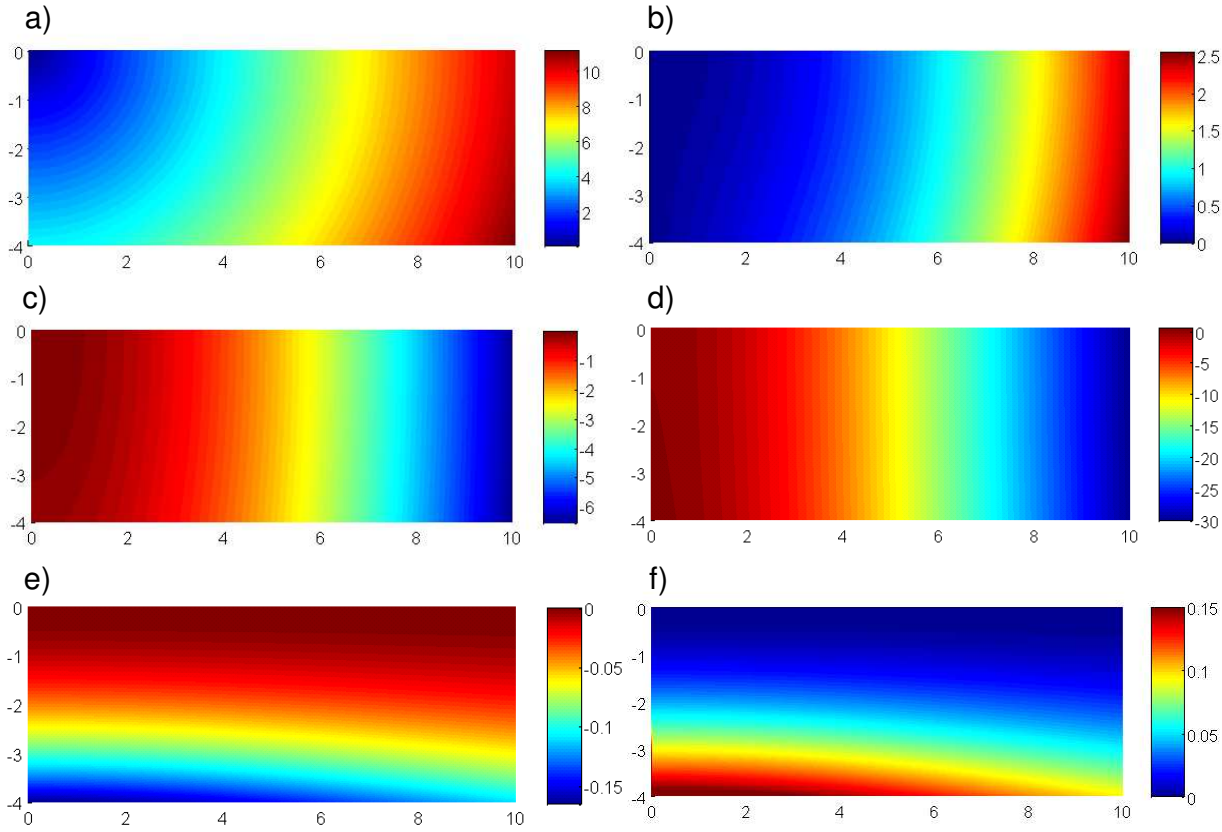

Figure 3. Complex travel time and its errors in model A. (a) real part of the exact travel time, τ^R, (b) imaginary part of the exact travel time, τ^I, (c) errors of τ^R produced by the elastic ray tracing, (d) errors of τ^I produced by the elastic ray tracing, (e) errors of τ^R produced by the viscoelastic ray tracing, (f) errors of τ^I produced by the viscoelastic ray tracing. The travel time (a-b) is in seconds, the errors of the travel time (c-f) are in %. The horizontal and vertical scales are in km.

Figure 3 shows the solutions of the complex eikonal equation using three methods: the real viscoelastic ray tracing, the complex ray tracing and the real elastic ray tracing with perturbations. To cover densely the region under study, the rays were shot from the source

at $\mathbf{x}_S = (0, 0)^T$ with incidence angles ranging from 0° to 90° with a step of 0.25º. The maximum distance between two consecutive points along a ray was 0.02 km. Plots 3a-b show the exact complex traveltime calculated using the complex ray tracing. Plots 3c-d show the errors of the real elastic ray approach and plots 3e-f show the errors of the real viscoelastic ray approach. The errors are calculated at each point of the model using the following formulas:

$$e_R = \frac{\left(\tau^{\text{exact}}\right)^R - \left(\tau^{\text{aprox}}\right)^R}{\left(\tau^{\text{exact}}\right)^R} 100\% \ , \ e_I = \frac{\left(\tau^{\text{exact}}\right)^I - \left(\tau^{\text{aprox}}\right)^I}{\left(\tau^{\text{exact}}\right)^I} 100\% \ . \tag{26}$$

Maximum errors of the complex traveltime calculated by the real viscoelastic ray tracing attain values up to 0.15%. The elastic ray tracing yields errors remarkably higher: up to 6% in τ^R, and up to 30% in τ^I.

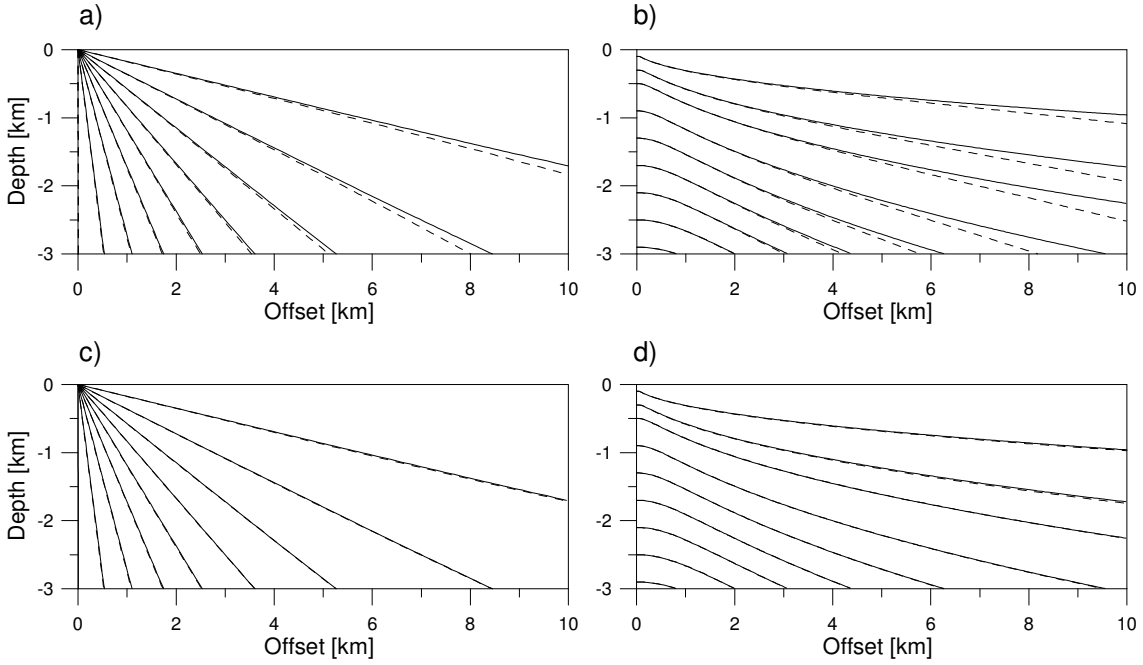

Figure 4. Ray fields in model A. Solid line - exact solution calculated using the complex ray tracing, dashed line – approximate solution calculated using the elastic ray tracing (a-b), and using the viscoelastic ray tracing (c-d). Left-hand plots show the propagation rays, right-hand plots show the attenuation rays. The propagation rays are shot at the origin of coordinates in incidences from 10º to 90º with a step of 10º. The attenuation rays are shot at $x = 0$ and z = –0.1, –0.3, –0.5, –0.9, –1.3, –1.7, –2.1, –2.5 and –2.9 km.

The errors in τ also influence the ray fields calculated from gradients of τ. Figure 4 shows the propagation (left-hand plots) and attenuation (right-hand plots) rays in model A. The rays were calculated as curves of the steepest ascent of the real and imaginary parts of the complex traveltime τ. The traveltime gradients were computed numerically using the finite differences. Since traveltime τ was calculated at a very dense grid of points in the studied region, the errors introduced by approximating the gradients by the finite differences are negligible. As expected, the propagation rays start at the point source situated at the origin of coordinates. The rays are close to the straight lines. However, the attenuation rays behave differently. The attenuation rays do not origin at the source, but at the vertical axis below the source.

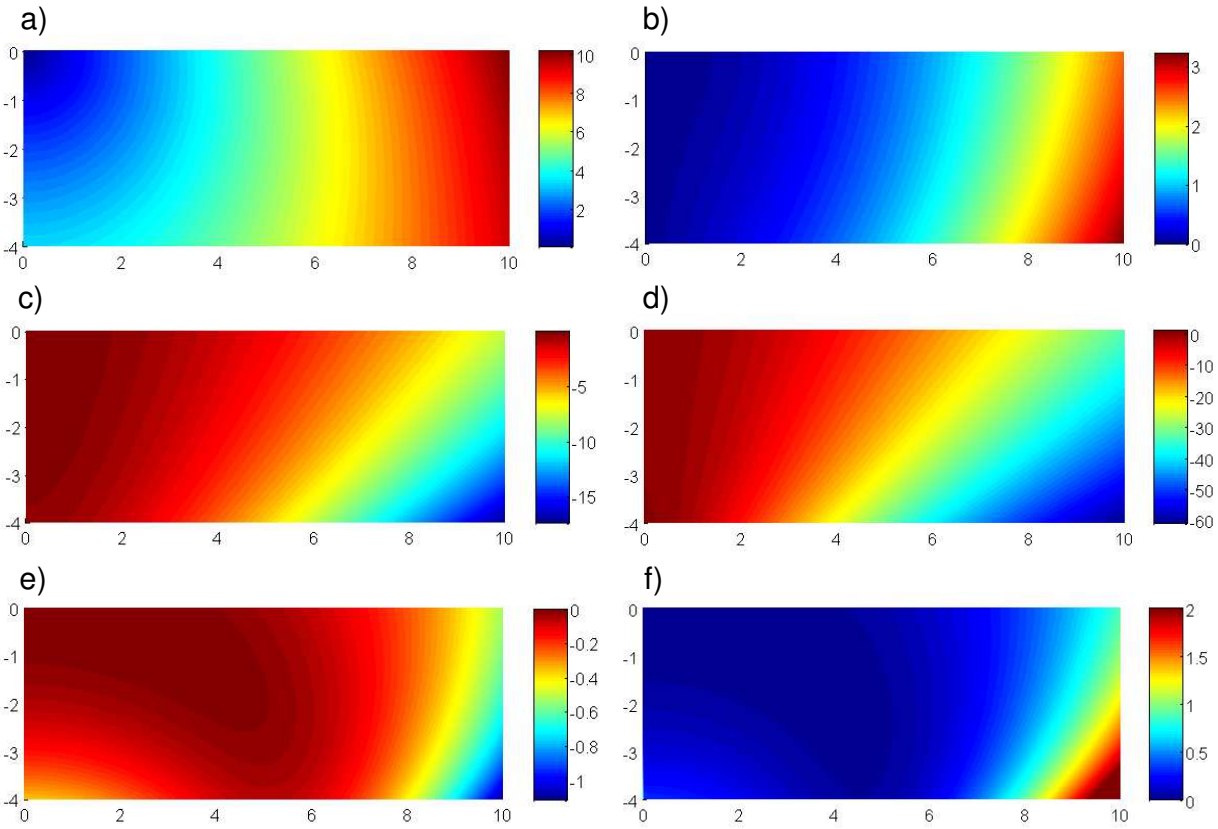

Figure 5. Complex travel time and its errors in model B. (a) real part of the exact travel time, τ^R, (b) imaginary part of the exact travel time, τ^I, (c) errors of τ^R produced by the elastic ray tracing, (d) errors of τ^I produced by the elastic ray tracing, (e) errors of τ^R produced by the viscoelastic ray tracing, (f) errors of τ^I produced by the viscoelastic ray tracing. The travel time (a-b) is in seconds, the errors of the travel time (c-f) are in %. The horizontal and vertical scales are in km.

The remarkable differences between the propagation and attenuation rays indicate that the slowness vector is inhomogeneous. Since the model is elastic at $x = 0$, the imaginary traveltime τ^I is zero along the whole left vertical border of the region under study. Consequently, the attenuation rays have the starting direction perpendicular to this border. The ray direction changes with the increasing traveltime and the attenuation rays form a family of smooth quasi-parallel curves. With the increasing traveltime, the approximate rays calculated by elastic ray tracing start to deviate from the exact rays. The differences are visible in the propagation as well as attenuation ray fields. On the contrary, the real viscoelastic ray tracing predicts ray fields identical to exact ones.

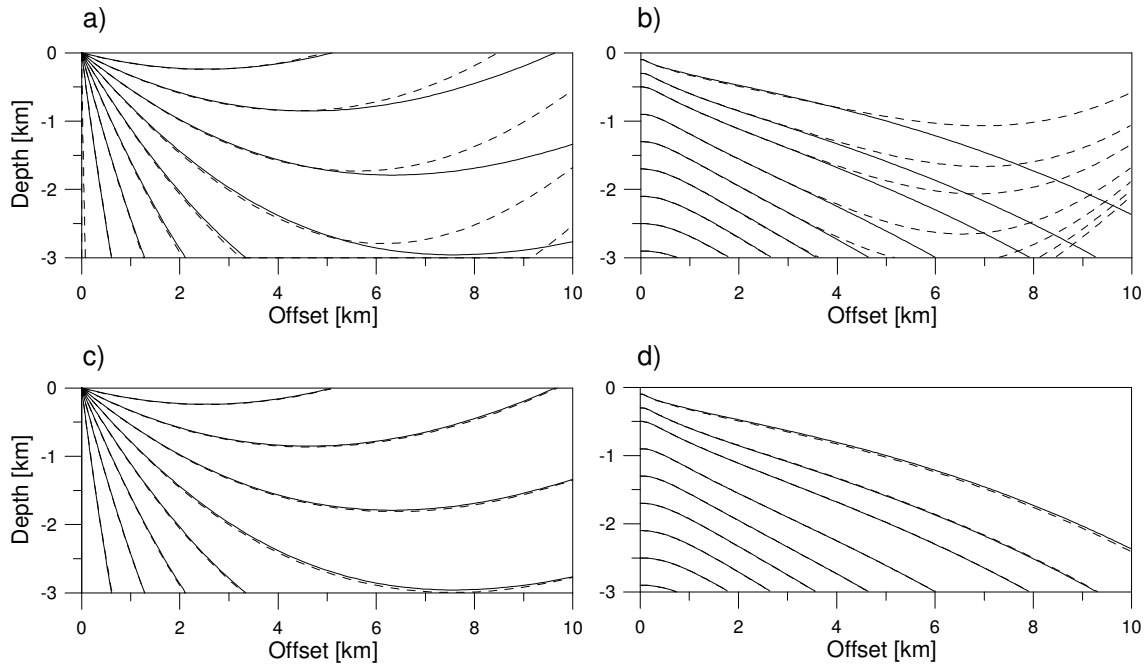

Figure 6. Ray fields in model B. Solid line - exact solution calculated using the complex ray tracing, dashed line – approximate solution calculated using the elastic ray tracing (a-b), and using the viscoelastic ray tracing (c-d). Left-hand plots show the propagation rays, right-hand plots show the attenuation rays. The propagation rays are shot at the origin of coordinates in incidences from 10º to 90º with a step of 10º. The attenuation rays are shot at $x = 0$ and z = –0.1, –0.3, –0.5, –0.9, –1.3, –1.7, –2.1, –2.5 and –2.9 km.

Figures 5 and 6 are analogous to Figs 3 and 4, but for model B. Since model B is more complicated than model A, the approximate methods work with a lower accuracy. Figure 5 indicates that the real elastic ray tracing yields errors in τ^R up to 15% and errors in τ^I up to 60%. The real viscoelastic ray tracing yields errors in τ^R up to 1% and in τ^I up

to 2%. The geometry of the propagation rays is distinctly distorted in the case of the elastic ray approach and completely fails for the attenuation rays (see Fig. 6). On the other hand, the real viscoelastic ray approach predicts the ray fields almost identical with the exact ones.

6. CONCLUSIONS

The numerical tests indicate that the real viscoelastic ray tracing proposed by Vavryčuk (2008a) is efficient and accurate. Compared with the complex ray tracing, which is complicated and limited to simple types of media only, the real viscoelastic ray tracing offers a fast and computationally undemanding procedure for calculating the complex travel times in 3-D inhomogeneous attenuating structures. The procedure works even for high velocity gradients and for strong attenuation. It yields accurate results even in models in which the standard elastic ray tracing fails.

The computational scheme of the real viscoelastic ray tracing in isotropic viscoelastic media is very similar to that in isotropic elastic media. Hence, existing computer codes working in purely elastic media can be simply generalized to attenuating media. In models with the Q-factor independent of frequency, the computational demands on the ray tracing are, in principle, the same as in the elastic case. In models of the frequency-dependent Q, the ray tracing procedure must be run repeatedly at different frequencies. The real viscoelastic ray tracing is also applicable to anisotropic viscoelastic media, but the procedure is computationally more demanding. In order the real viscoelastic ray approach to be applicable to calculating rays in realistic structures, additional equations for transforming rays at interfaces must be accomplished.

ACKNOWLEDGMENTS

I thank Luděk Klimeš and two anonymous reviewers for their comments. The work was supported by the Grant Agency of the Academy of Sciences of the Czech Republic, Grant No. IAA300120801, and by the Consortium Project “Seismic Waves in Complex 3-D Structures”.

REFERENCES

Amodei, D., Keers, H., Vasco, W. & Johnson, L., 2006. Computation of uniform wave forms using complex rays, *Physical Review E*, **73**, 036704, 1-14.

Auld, B.A., 1973. *Acoustic Fields and Waves in Solids*, Wiley, New York.

Bulant, P. & Klimeš, L., 2002. Numerical algorithm of the coupling ray theory in weakly anisotropic media, *Pure Appl. Geophys.*, **159**, 1419-1435.

Carcione, J.M., 1990. Wave propagation in anisotropic linear viscoelastic media: theory and simulated wavefields, *Geophys. J. Int.*, **101**, 739-750. Erratum: 1992, **111**, 191.

Carcione, J.M., 2007. *Wave Fields in Real Media: Theory and Numerical Simulation of Wave Propagation in Anisotropic, Anelastic, Porous and Electromagnetic Media*, Elsevier, Amsterdam.

Caviglia, G. & Morro, A., 1992. *Inhomogeneous Waves in Solids and Fluids*, World Scientific, London.

Červený, V., 2001. *Seismic Ray Theory*, Cambridge University Press, Cambridge, U.K.

Červený, V., 2002. Fermat's variational principle for anisotropic inhomogeneous media, *Stud. Geophys. Geod.*, **46**, 567-588.

Červený, V., Klimeš, L. & Pšenčík, I., 2008. Attenuation vector in heterogeneous, weakly dissipative, anisotropic media, *Geophys. J. Int.*, **175**, 346-355.

Červený, V. & Pšenčík, I., 2008. Perturbation Hamiltonians in heterogeneous anisotropic weakly dissipative media, in *Seismic Waves in Complex 3-D Structures*, Report **18**, Dep. Geophys., Charles Univ., Prague, pp. 223-244.

Chapman, S.J., Lawry, J.M.H., Ockendon, J.R. & Tew, R.H., 1999. On the theory of complex rays, *SIAM Review*, **41**, 417-509.

Gajewski, D. & Pšenčík, I., 1992. Vector wavefield for weakly attenuating anisotropic media by the ray method, *Geophysics*, **57**, 27-38.

Hanyga, A. & Seredyňska, M., 1999. Asymptotic ray theory in poro- and viscoelastic media, *Wave Motion*, **30**, 175-195.

Hanyga, A. & Seredyňska, M., 2000. Ray tracing in elastic and viscoelastic media, *Pure Appl. Geophys.*, **157**, 679-717.

Kiselev, A.P., 1993. Ray theory of modulated body waves in inhomogeneous viscoelastic media, *Pure Appl. Geophys.*, **140**, 629-640.

Klimeš, L., 2002. Second-order and higher-order perturbations of travel time in isotropic and anisotropic media, *Stud. Geophys. Geod.*, **46**, 213-248.

Kravtsov, Yu.A., 2005. *Geometrical Optics in Engineering Physics*, Alpha Science, Harrow, U.K.

Kravtsov, Yu.A., Forbes, G.W. & Asatryan, A.A., 1999. Theory and applications of complex rays, in *Progress in Optics*, ed. E. Wolf (Amsterdam, Elsevier 1999), vol. 39, pp. 3-62.

Moczo, P., Kristek, J. & Halada, L., 2004. *The Finite-Difference Method for Seismologists. An Introduction*, Comenius University, Bratislava. (158 pp., ISBN 80-223-2000-5).

Moczo, P., Kristek, J., Gális, M., Pažák, P. & Balazovjech, M., 2007. The finite-difference and finite-element modeling of seismic wave propagation and earthquake motion, *Acta Physica Slovaca*, **57**(2), 177-406.

Ribodetti, A. & Virieux, J., 1998. Asymptotic theory for imaging the attenuation factor Q, *Geophysics*, **63**, 1767-1778.

Saenger, E.H., & Bohlen, T., 2004. Finite-difference modeling of viscoelastic and anisotropic wave propagation using the rotated staggered grid, *Geophysics*, **69**, 583-591, doi:10.1190/1.1707078.

Thomson, C.J., 1997. Complex rays and wave packets for decaying signals in inhomogeneous, anisotropic and anelastic media, *Stud. Geophys. Geod.*, 41, 345-381.

Vavryčuk, V., 2007a. Asymptotic Green's function in homogeneous anisotropic viscoelastic media, *Proc. Roy. Soc.*, **A 463**, 2689-2707, doi:10.1098/rspa.2007.1862.

Vavryčuk, V., 2007b. Ray velocity and ray attenuation in homogeneous anisotropic viscoelastic media, *Geophysics*, **72**, D119-D127, doi:10.1190/1.2768402.

Vavryčuk, V., 2008a. Real ray tracing in anisotropic viscoelastic media, *Geophys. J. Int.*, **175**, 617-626, doi: 10.1111/j.1365-246X.2008.03898.x.

Vavryčuk, V., 2008b. Velocity, attenuation and quality factor in anisotropic viscoelastic media: a perturbation approach, *Geophysics*, **73**, No. 5, D63-D73, doi: 10.1190 /1.2921778.

Appendix A: Analytic complex ray tracing in a medium with a constant gradient of c^{-2}

Similarly as for the real ray tracing in elastic media (see Červený 2001, Sec. 3.4), the simplest analytical solution of the complex ray tracing is obtained for a medium with a constant gradient of the square of slowness c^{-2}. Let us assume that c^{-2} is given by

$$c^{-2}(\mathbf{x}) = c_0^{-2} + A_i x_i \,, \tag{A1}$$

and consider only that part of the space where $\left(c^{-2}\right)^R > 0$. All quantities in (A1) are generally complex. The ray tracing equations (20) yield the following solution

$$x_i(\sigma) = x_{i0} + p_{i0}(\sigma - \sigma_0) + \frac{1}{4} A_i (\sigma - \sigma_0)^2 , \tag{A2}$$

$$p_i(\sigma) = p_{i0} + \frac{1}{2} A_i (\sigma - \sigma_0) , \tag{A3}$$

$$\tau(\sigma) = \tau_0 + c_0^{-2}(\sigma - \sigma_0) + \frac{1}{2} A_i p_{i0} (\sigma - \sigma_0)^2 + \frac{1}{12} A_i A_i (\sigma - \sigma_0)^3 , \tag{A4}$$

where σ is the complex parameter along the ray. Let us assume the point source at the centre of the coordinates and zero parameter σ at the source:

$$\mathbf{x}_0 = (0,0,0)^T , \ \sigma_0 = 0 . \tag{A5}$$

The receiver lies in the real space having coordinates $\mathbf{x}^R = \left(x_1^R, x_2^R, x_3^R\right)^T$. Equation (A2) together with the eikonal equation at the source,

$$p_{i0} p_{i0} = c_0^{-2} , \tag{A6}$$

represent a system of four complex equations for four complex unknowns: p_{10}, p_{20}, p_{30} and σ. Eliminating slowness components p_{10}, p_{20} and p_{30}, we obtain the quadratic equation for σ^2,

$$\frac{1}{16} A_i A_i \sigma^4 - \left(p_0^2 + \frac{1}{2} A_i x_i^R \right) \sigma^2 + x_i^R x_i^R = 0 . \tag{A7}$$

Solving this equation for σ, we can evaluate from (A2-A4) the slowness vector $\mathbf{p}_0$ at the source $\mathbf{x}_0$, slowness vector $\mathbf{p}(\mathbf{x}^R)$ at the receiver $\mathbf{x}^R$, and traveltime at the receiver $\tau(\mathbf{x}^R)$.